

Characterization of Stretchable Serpentine Microwave Devices for Wearable Electronics

Tammy Chang¹, Casey Wojcik¹, Yewang Su², John A. Rogers³, Thomas H. Lee¹, and Jonathan A. Fan¹

¹Stanford University, Stanford, CA 94305 USA

²Chinese Academy of Sciences & University of Chinese Academy of Sciences, Beijing, 100049 CN

³Northwestern University, Evanston, IL 60208 USA

Abstract— Serpentine interconnects, made stretchable by patterning copper traces into serpentine mesh geometries, are attractive for applications in wearable electronics. This paper studies the suitability of these structures for wireless devices at microwave frequencies, where the sub-wavelength dimensions of the serpentine pattern contribute to changes in electrical length and propagation loss. The effects of converting solid metal traces to serpentine geometries are quantified for microwave transmission lines and dipole antennas. In addition, the effects of stretching are characterized and measured for a fabricated dipole antenna.

Index Terms—Serpentine mesh, stretchable, conformal, wearable electronics.

I. INTRODUCTION

Stretchable electronics have been viewed as a core technology for wearable health monitoring systems, especially for systems where electronics are applied directly to skin [1]. For stretchable wireless designs, methods used for highly stretchable microwave devices have included the use of materials composites, such as silver nanowires embedded in elastomeric substrates [2], as well as structural approaches, such as the patterning of metal sheets into serpentine designs, followed by bonding to elastomeric substrates [1], [3]–[5]. The former approach is typically high in loss, producing conductors with conductivities no greater than 10^4 S/cm. The latter approach, which is the focus here, enables the use of high-quality metals such as copper, thereby allowing high performance, low-loss devices. While the stretchable mechanics of this approach have been characterized [3], the impact of the serpentine geometry on microwave device properties has not been previously studied in detail.

In this paper, we investigate the properties of stretchable serpentine microwave devices. Section II introduces the serpentine design concept and studies the microwave effects introduced by converting a solid metal design into a serpentine mesh design. Section III focuses on the effects of stretching and includes the fabrication process and measured results for a fabricated dipole antenna.

II. MICROWAVE EFFECTS OF SERPENTINE STRUCTURE

Stretchable serpentine designs have undergone progressive development over recent years. Fundamentally, metallic interconnects are designed in a curvilinear fashion and

fabricated on an elastic substrate so that they can yield scissor-like deformations when strained [1,2]. A microwave device designed using this method is shown in Fig. 1(a).

A. Conversion from Solid to Serpentine

To convert a solid structure to a stretchable serpentine, it can be replaced with a sub-wavelength rectangular mesh, as shown in Fig. 2(a)-(b) for a half-wavelength dipole. The device becomes stretchable when the meshed lines are replaced with circular arcs of angle θ_{arc} , as shown in Fig. 1(b). As the arc angle progressively increases between adjacent nodes (Fig. 2(c)-(e)), stretchability increases as well. Although the serpentine structure undergoes a sub-wavelength structural change (the mesh spacing s_{mesh} is approximately 1/70 of the free-space wavelength, λ_0), the added curvature changes the propagation of surface current, as will be discussed in the following subsection.

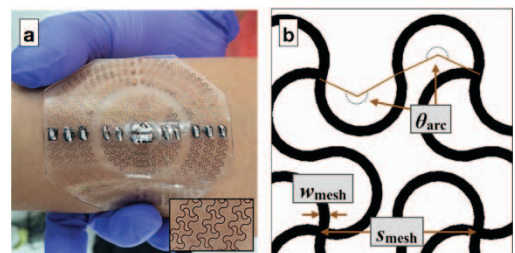


Fig. 1. (a) Microwave transmitter made of serpentine interconnects and surface-mount components for wearable applications. (b) Close-up diagram of serpentine dimensions.

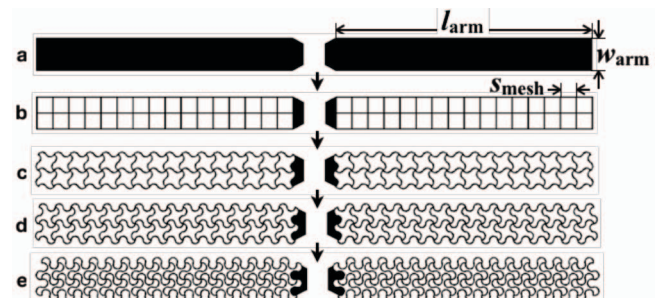


Fig. 2. Conversion of dipole antenna from solid to rectangular mesh, and then to serpentine mesh as the angle of curvature is increased. From top to bottom: (a) solid, (b) rectangular mesh, serpentines with (c) $\theta_{arc} = 120^\circ$ (d) $\theta_{arc} = 170^\circ$, and (e) $\theta_{arc} = 220^\circ$.

B. Characterization of Serpentine Structure

We utilize a microstrip transmission line setup in Ansoft HFSS to study microwave propagation along the serpentine structure. Four different types of mesh structures, each with different serpentine arc angles, are simulated and compared with a solid microstrip transmission line. The transmission lines are simulated with 32 μm copper traces on a 1.8 mm thick PDMS (polydimethylsiloxane) substrate ($\epsilon_r = 3$ and $\tan\delta = 0.014$ [6]). The surface current distribution in Fig. 3(a), shows propagation occurring primarily along the horizontal direction of the transmission line, which is consistent with prior findings for meshed antennas without the serpentine arc [7]. Simulations of surface current with the serpentine arc in Fig. 3(b)-(d) show that even with increasing θ_{arc} , propagation follows a similar trend in the horizontal direction. These results indicate that, despite intersections between the traces in the serpentine mesh, the serpentine mesh acts much like a meander line, as little to no current travels through the vertical traces.

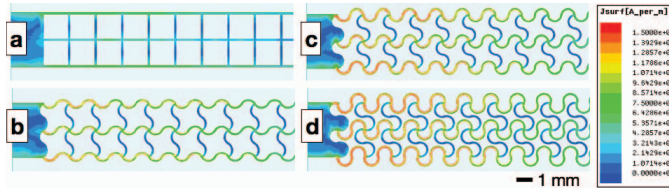


Fig. 3. Simulated surface current magnitude at 1.6 GHz for four different microstrip transmission lines on PDMS substrates.

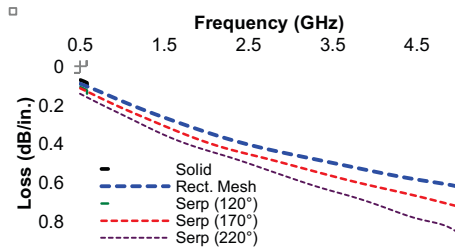


Fig. 4. Transmission line loss for solid, rectangular, and serpentine structures shown in Fig. 3.

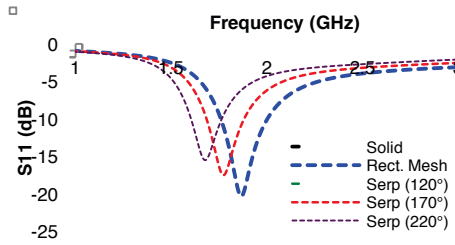


Fig. 5. S11 for solid, rectangular, and serpentine dipole antennas.

The plot of simulated transmission in Fig. 4 shows loss increasing by 0.1 dB/in to 0.3 dB/in at 2.5 and 5 GHz as the serpentine arc angle increases. This loss is likely due to the greater trace length resulting from the curvature between adjacent nodes. The serpentine arc could also cause coupling of fields along the line and contribute to the propagation loss.

We also note that the loss relationship is not linear with increasing arc angle, as there is a greater decrease in loss from 170° to 220° than from 120° to 170°.

Similar effects are also observed when meshing is applied to dipole antennas, as shown in Fig. 2. The dipoles have an arm length and width of $l_{\text{arm}} = 24.5$ mm and $w_{\text{arm}} = 3.41$ mm, and mesh spacing and width of $s_{\text{mesh}} = 1.65$ mm and $w_{\text{mesh}} = 0.11$ mm. The antennas are mounted on a 60 mm x 16 mm PDMS substrate. From the return loss results shown in Fig. 5, the electrical length increases as the structure changes from solid to serpentine, similar to a meander line, as evidenced by a 12% decrease in resonant frequency from 1.91 to 1.68 GHz. Loss behavior similar to that observed in Fig. 4 is also evident from the decrease in radiation efficiency at resonance from 96.5% to 93%, as shown in Table I.

TABLE I
DIPOLE RADIATION EFFICIENCY FOR DIFFERENT STRUCTURES

Antenna	Resonant Freq. (GHz)	Efficiency (%)
Solid	1.91	96.5
Rectangular Mesh	1.87	95.6
Serpentine (120°)	1.83	94.6
Serpentine (170°)	1.77	94.1
Serpentine (220°)	1.68	93.0

III. MICROWAVE EFFECTS DUE TO STRETCHING

The previous section discussed the serpentine structure itself; this section will investigate the effects of stretching on microwave performance.

A. Fabrication of Stretchable Serpentine Devices

To fabricate stretchable serpentine structures, photolithography was used to pattern the serpentine designs from a copper sheet with a thickness of 32 μm (Fig. 2(a)-(b)). The patterned device was then evaporated with silica (SiO_2) and bonded to PDMS (polydimethylsiloxane) using plasma treatment (Fig. 2(c)-(e)). Once the bonding was finished, a protective coating layer of PDMS was applied (Fig. 2(f)).

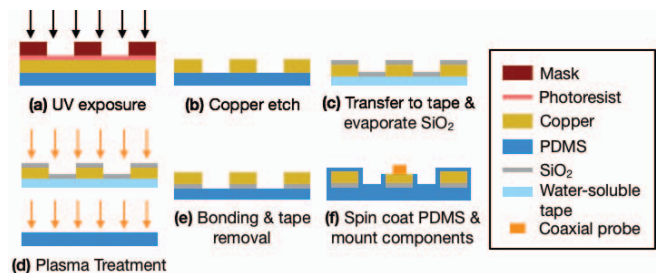


Fig. 6. Simplified schematic of fabrication process.

B. Characterization of Stretching

To characterize the mechanical characteristics of fabricated devices, simulations of stretching were performed in ABAQUS software. Figure 7 shows the stress at a 30%

stretch. The stress is highest near the center of the serpentine arc and at the intersections of traces. It is also evident that the overall shape of the serpentine structure increases in length and decreases in width; this observation is helpful for modeling uniaxial stretching in electromagnetic simulations.

To confirm simulations, a serpentine dipole antenna was fabricated with 220° arc angle and the same dimensions described in Section II, as shown in Fig. 8. Uniaxial stretching was applied to the two short edges of the antenna's elastomer substrate, and the measured return losses are shown in Fig. 9. The measured resonant frequency decreases from 1.7 to 1.37 GHz (19% decrease) for 30% stretching, matching closely with simulated results where the resonant frequency decreases from 1.68 to 1.37 GHz.

In addition, far-field measurements of the antenna pattern were conducted for 0% and 20% stretching at 1.7 and 1.56 GHz, respectively. These results are shown in Fig. 10. Overall, the radiation pattern maintains the same profile, even after stretching, with a minor increase in gain for the E-plane pattern from 2 to 2.5 dBi (this could be due in part to an increase in radiation efficiency after stretching, which is also evident in the simulated results shown in Table II). The cross-polarization suppression ranges from 10 to 15 dB, showing that the dipole emits a linearly polarized field despite the serpentine mesh.

IV. CONCLUSION

The results discussed in this paper show that increasing stretchability with the serpentine mesh results in changes to resonant length and increased loss along the structure. However, the resulting loss from converting solid to serpentine is on the order of 5%, and the changes in resonant length can be accommodated by a 10-15% reduction in unstretched length. Stretching the serpentine structure also changes resonant length by 19% for 30% stretching, but does not significantly change the radiation pattern of a fabricated dipole antenna. These results of stretching indicate that changes to resonant length must be characterized in order to implement serpentine microwave devices in robust systems.

ACKNOWLEDGMENT

The authors would like to acknowledge Dan Gregoire and Calvin Yang for their assistance in measurements and simulations for this work. This work is supported in part by the Department of Defense (DoD) through the National Defense Science & Engineering Fellowship (NDSEG) Program.

REFERENCES

- [1] L. Song, A. C. Myers, J. J. Adams, Y. Zhu, "Stretchable and Reversibly Deformable Radio Frequency Antennas Based on Silver Nanowires," *ACS Applied Materials & Interfaces*, vol. 6, no. 6, pp. 4248-4253, Mar. 2014.
- [2] D. Kim, N. Lu, R. Ma et al., "Epidermal Electronics," *Science*, vol. 333, pp. 838-844, Aug. 2011.
- [3] Y. Su, X. Ping, K. J. Yu et al., "In-Plane Deformation Mechanics for Highly Stretchable Electronics," *Advanced Materials*, accepted Nov. 2016.
- [4] J. Fan, W. Yeo, Y. Su et al., "Fractal Design Concepts for Stretchable Electronics," *Nature Communications*, vol. 5, no. 3266, Feb. 2014.
- [5] T. Jang, C. Zhang, H. Youn, J. Zhou, L. J. Guo, "Transparent and Flexible Mechanically Reconfigurable Electrically Small Antennas Based on Tortuous Metallic Micromesh," *IEEE Transactions on Antennas and Propagation*, no. 99, Nov. 2016.
- [6] J. Castro, T. Weller, J. Wang, "An Improved Fabrication Method of High-k and Low-loss Polymer Composites with Sintered Ceramic Fillers for Microwave Applications," 2015 *IEEE MTT-S Int. Microw. Symp. Dig.*, Phoenix, AZ, USA, May 2015.
- [7] T. W. Turpin, R. Baktur, "Meshed Patch Antennas Integrated on Solar Cells," *IEEE Antennas and Wireless Propagation Letters*, vol. 8, pp. 693-696, Jun. 2009.

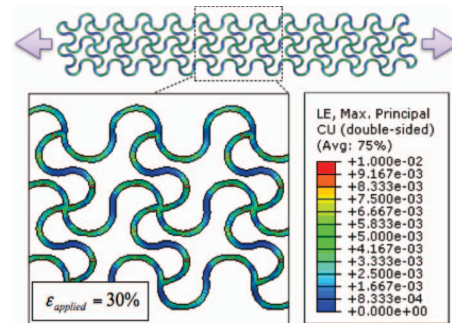


Fig. 7. Distribution of stress for 30% stretching of the serpentine substrate.



Fig. 8. Fabricated stretchable dipole antenna.

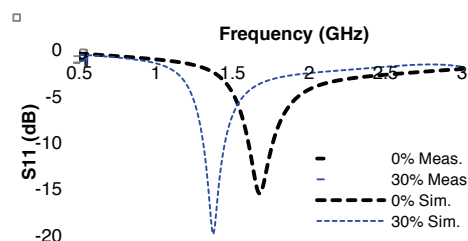


Fig. 9. Simulated and measured return loss for the fabricated dipole antenna.

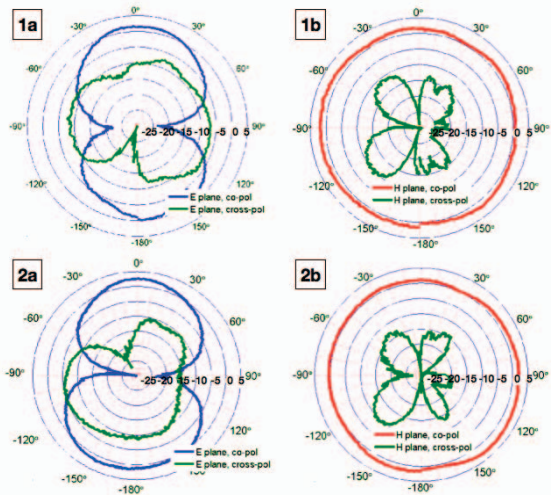


Fig. 10. Measured dipole radiation pattern for 0% stretching (1(a)-(b)) and 20% stretching (2(a)-(b)).

TABLE II
DIPOLE RADIATION EFFICIENCY WITH STRETCHING

Stretching	Resonant Freq. (GHz)	Efficiency (%)
0%	1.68	93.0
30%	1.37	93.7